



## Molecular Crystals and Liquid Crystals Science and Technology. Section A. Molecular Crystals and Liquid Crystals

Publication details, including instructions for authors and subscription information:

<http://www.tandfonline.com/loi/gmcl19>

### FT-IR and FT-Raman Spectroscopic Studies of 1-(p-n-Alkyl Phenyl) 3-(p-n-Alkyloxyphenyl) Propane 1,3-Diones

P. Raveendran<sup>a</sup>, B. K. Sadashiva<sup>b</sup>, K. V.G.K. Murty<sup>a</sup> & T. K. K. Srinivasan<sup>a</sup>

<sup>a</sup> Regional Sophisticated Instrumentation Centre, Department of Chemistry, Indian Institute of Technology, Madras, INDIA, 600 036

<sup>b</sup> Raman Research Institute, Bangalore, INDIA, 560 080

Version of record first published: 24 Sep 2006

To cite this article: P. Raveendran, B. K. Sadashiva, K. V.G.K. Murty & T. K. K. Srinivasan (2001): FT-IR and FT-Raman Spectroscopic Studies of 1-(p-n-Alkyl Phenyl) 3-(p-n-Alkyloxyphenyl) Propane 1,3-Diones, *Molecular Crystals and Liquid Crystals Science and Technology. Section A. Molecular Crystals and Liquid Crystals*, 363:1, 19-34

To link to this article: <http://dx.doi.org/10.1080/10587250108025255>

PLEASE SCROLL DOWN FOR ARTICLE

Full terms and conditions of use: <http://www.tandfonline.com/page/terms-and-conditions>

This article may be used for research, teaching, and private study purposes. Any substantial or systematic reproduction, redistribution, reselling, loan, sub-licensing, systematic supply, or distribution in any form to anyone is expressly forbidden.

The publisher does not give any warranty express or implied or make any representation that the contents will be complete or accurate or up to date. The accuracy of any instructions, formulae, and drug doses should be independently verified with primary sources. The publisher shall not be liable for any loss, actions, claims, proceedings, demand, or costs or damages whatsoever or howsoever caused arising directly or indirectly in connection with or arising out of the use of this material.

# FT-IR and FT-Raman Spectroscopic Studies of 1-(*p-n*-Alkyl Phenyl) 3-(*p-n*-Alkyloxyphenyl) Propane 1,3-Diones

P. RAVEENDRAN<sup>a</sup>, B.K. SADASHIVA<sup>b</sup>, K.V.G.K. MURTY<sup>a</sup> and T.K.K. SRINIVASAN<sup>a\*</sup>

<sup>a</sup>Regional Sophisticated Instrumentation Centre, Department of Chemistry, Indian Institute of Technology, Madras, INDIA – 600 036 and <sup>b</sup>Raman Research Institute, Bangalore, INDIA-560 080

(Received June 13, 2000)

FT-IR and FT-Raman spectroscopic studies of the mesogens with the general molecular formula 1-(*p-n*-alkyl phenyl) 3-(*p-n*-alkyloxyphenyl) propane 1,3-diones having alkyl chain lengths C<sub>10</sub>, C<sub>11</sub> and C<sub>12</sub> are carried out. An analysis of the vibrational spectra of C<sub>10</sub>, C<sub>11</sub> and C<sub>12</sub> at room temperature strongly suggests that while C<sub>12</sub> probably belongs to a highly ordered monoclinic or orthorhombic type of lattice, C<sub>10</sub> and C<sub>11</sub> belong to a hexagonal or triclinic unit cell, having lesser degree of lattice order.

## 1. INTRODUCTION

The structural features associated with the physical properties of liquid crystals have been an interesting topic of research for over three decades by now and considerable efforts have been underway to characterise the structural differences<sup>1-9</sup>. Majority of the known mesogens possess both planar aromatic rings and long flexible alkyl chains. Vibrational spectroscopic structure determination methods provide almost independent experimental measures of both the ordering of the alkyl chains and the aromatic part of the molecule. Investigations of the disorder in the alkyl chains is mainly based on the extensive vibrational spectroscopic studies by Snyder<sup>10-16</sup> and coworkers<sup>17-22</sup> on *n*-alkanes. Vibrational spectro-

\* Address for Communication.

scopic structural investigation of alkyl chain disorder is mainly based on the analysis of the conformational sensitive methylene group vibrations and the C-H stretching region of the spectra which undergo Fermi resonance interaction with the methylene bending modes. The intensity and splitting of these bands also depend on the packing of the chains in the lattice and thus provide information regarding the crystal structure differences in the various systems.

Vibrational spectroscopic analysis of the mesogens with the general molecular formula 1-(p-n-alkyl phenyl) 3-(p-n-alkyloxyphenyl) propane 1,3-diones is very interesting. These molecules undergo keto-enol tautomerism (Fig. 1) as observed generally in the  $\beta$ -diketones<sup>24,25</sup> and primarily exist in the enol form. The formation of mesophases in these systems is highly dependent on the length of the alkyl chain. The homologues with alkyl chain length upto C<sub>9</sub> do not exhibit mesophases, and directly transform from the solid crystalline to the isotropic liquid phase. The higher homologues exhibit mesomorphism<sup>24</sup>.

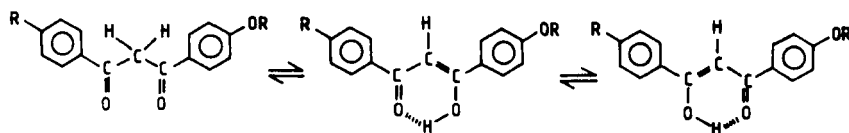


FIGURE 1 Keto-enol tautomerism in the mesogens with the general molecular formula 1-(p-n-alkyl phenyl) 3-(p-n-alkyl oxyphenyl) propane 1,3-diones

In the present work, mesogens of the above-mentioned series of alkyl chain lengths 10, 11, and 12, denoted as C<sub>10</sub>, C<sub>11</sub> and C<sub>12</sub> respectively are chosen. The crystal structures of these mesogens are not reported so far. These investigations are aimed at the vibrational spectroscopic characterization of the crystal structure differences among the three homologues (in view of the lack of crystal structure of these systems), and the extent of alkyl chain disorder in these systems.

## 2. SOME THEORETICAL ASPECTS

The various vibrational modes of the methylene and methyl vibrational modes can be used to probe the alkyl chain disorder, in general. For alkyl chains with 'n' atoms per repeat unit and M repeat units, there are 3n modes of vibration, which occur in 3n frequency branches. Within each branch, the frequency of each of the M possible modes depends upon the relative phase of the nuclear displacements of the neighbouring units, each mode being characterised by a phase angle  $\varphi_k = K \pi/M$ , with  $K = 0, 1, \dots, M-1$ . For an infinite polymer such as polyethylene

only those modes with  $K=0$  are allowed both in the IR and Raman spectra (i.e. the vibration in each repeat unit are totally in phase). For segments of chains that are less than infinite in length, or disordered due to 'gauche' rotamer formation, the above selection rules are not vigorous, and the vibrations corresponding to other  $K$ -values also will become active. The frequency of certain vibrations with  $K=0$  will be a function of the all-trans segment length present in the  $\text{CH}_2$  oligomer, thus providing useful structural probes in systems with long alkyl chains.

The various vibrational modes of the hydrocarbon chain are designated according to Snyder<sup>15</sup> as follows:  $d^+$  and  $d^-$  are the symmetric and antisymmetric C-H stretching modes of the methylene symmetric group respectively,  $r^+$  and  $r^-$  are the symmetric and asymmetric (degenerate) methyl C-H stretching,  $\delta$  is the HCH bending mode and P denotes the methyl rocking mode. In an ordered infinite chain, methylene modes exist for all values of the phase angle ( $\phi$ ). For these modes to appear in the spectra, the value of  $\phi$  must be 0 or  $\pi$ . Thus  $d_{\pm}(0)$  and  $\delta(0)$  are the Raman active fundamentals and  $d_{\pm}(\pi)$  and  $\delta(\pi)$  are the IR active fundamentals<sup>15</sup>. It is found that the C-H stretching modes as well as the HCH bending modes of the methylene group have nearly similar dispersion in the liquid and in the crystal.

TABLE I Assignment of the various vibrational nodes of the alkyl chain

Frequency of IR active Modes ( $\text{cm}^{-1}$ )					Frequency of Raman active Modes ( $\text{cm}^{-1}$ )				
Mode	$C_{10}$	$C_{11}$	$C_{12}$	Assignment	Mode	$C_{10}$	$C_{11}$	$C_{12}$	Assignment
$d^-(\pi)$	2920	2920	2923	Antisym. C-H stretch ( $\text{CH}_2$ )	$d^-(0)$	2882	2882	2882	Antisym. C-H stretch ( $\text{CH}_2$ )
$r^+$	2860	2860	2860	Sym. C-H stretch ( $\text{CH}_3$ )	$r^+$	2860	2860	2860	Sym. C-H stretch ( $\text{CH}_3$ )
$d^+(\pi)$	2850	2850	2850	Sym. C-H stretch ( $\text{CH}_2$ )	$r^-$	2956	2958	2960	Antisym. C-H stretch ( $\text{CH}_3$ )
$r^-$	2956	2955	2954	Asym. C-H stretch ( $\text{CH}_3$ )	$d^+(0)$	2848	2848	2848	Sym. C-H stretch ( $\text{CH}_2$ )
$\delta(\pi)$	1468	1468	1471, 1463	$\text{CH}_2$ bending	$\delta(0)$	1454	1454	1454	$\text{CH}_2$ bending
P	738	735	729 719	$\text{CH}_2$ rock					

### C-H Stretching Modes

The symmetric and anti-symmetric methylene C-H stretch modes of a polymethylene chain<sup>25,26</sup> in the Raman spectrum appear around  $2850 \text{ cm}^{-1}$  and  $2880 \text{ cm}^{-1}$  respectively. On the other hand, the corresponding methylene bands in IR appear around  $2850 \text{ cm}^{-1}$  and  $2920 \text{ cm}^{-1}$  respectively. The  $\text{CH}_3$  symmetric

stretch mode( $r^+$ ) appear in both IR and Raman at around  $2870\text{ cm}^{-1}$ , where as the in-plane ( $r_a^-$ ) and out of plane ( $r_b^-$ ) asymmetric stretch modes appear at around  $2962\text{ cm}^{-1}$  and  $2950\text{ cm}^{-1}$  respectively. This region is usually the strongest feature in both the IR and Raman spectra of compounds containing long alkyl chains. The tentative assignment of the vibrational modes is presented in table I and II.

TABLE II Assignment of the various other vibrational modes of the FT-IR and FT-Raman spectra of  $C_{10}$ ,  $C_{10}$  and  $C_{12}$

$C_{10}$		$C_{11}$		$C_{12}$		Assignment
IR	Raman	IR	Raman	IR	Raman	
3062	3071	3062	3068	3070	3073	Aromatic C – H stretch
3028(vw)	3028	3027	–	3028	–	C – H {(CO-CH <sub>2</sub> -CO) region}
1605	1609	1605	1609	1605	1609	Phenyl ring stretch
1585	–	1585	–	1587	–	
1545	1545	1547	1547	1547	1530	Chelate ring modes
1504	1515	1503	1511	1513	1508	
1468	1454	1468	1554	1471	–	CH <sub>2</sub> bend
–	1436	–	1436	–	1443	19b (benzene ring)
1393	–	1393	–	1393	1394	(CH <sub>3</sub> ) wag progression
1377	–	1377	–	–	1362	CH <sub>2</sub> wag progression
1304	–	1305	–	1309	–	
–	1289	–	1280	–	1295	Q <sub>4</sub> (C – C) of the COCH <sub>2</sub> CO region
1258	–	1257	–	1254	1261	CH <sub>2</sub> wag progression
1228	–	1228	–	1226	1229	Aryl C-O stretch
1178	1180	1178	1182	1175	1178	$\phi$ – O-C stretch
1122	1129	1121	1122	1117	1121	C-C stretch
1089	1089	1090	–	–	1094	
–	1062	–	1063	–	1061	
1047	–	1051	–	1034	–	
1017	1020	1021	–	1020	1020	C (alkyl) – O stretch
990	974	984	–	1005	1006	$\phi$ – ring breathing modes
889	895	889	–	890	890	CH <sub>3</sub> rock
842 (Sh)	838	843	–	849	850	O-CH <sub>2</sub> rock
780	783	782	783	–	791	CH <sub>3</sub> CH <sub>2</sub> -rock, $\phi$ -C-H deformation(?)
738	741	735	–	729	746	CH <sub>2</sub> rock
719	–	719	–	719	–	
649	644, 650 (Sh)	648	650	655	655	Ring in-plane def.
633	636 m (Sh)	633	636 m (Sh)	633	633 m (Sh)	Ring out-of-plane def.
600	600	600	600	600	–	Ring in-plane def.
506	511	506	506	506	504	Ring in-plane def.

Although the C-H stretching modes are considered to be highly localised and relatively insensitive to molecular conformation and intermolecular packing in comparison with the methylene bending and rocking modes, Snyder and others<sup>25</sup> established a strong correlation between the relative intensity values of the various bands in this region to the intermolecular and intramolecular order in the alkyl chains. This correlation primarily emerges from the Fermi resonance interaction between the C – H stretch modes and the overtones of the methylene scissoring modes of the polymethylene chains. The methylene bending modes involved in the resonance interaction are sensitive to both molecular conformation and lateral inter-chain interactions. Moreover, it is known that unlike the C-H stretches, the bending modes tend to undergo significant intermolecular coupling. One can distinguish two levels of Fermi resonance interaction. The first one involves the dispersion of bending modes parallel to the chain axis. This interaction occurs in the completely isolated chains. The second, whose effects are similar to the first but distinguishable, is the intermolecular interaction and involves the perpendicular dispersion of the bending modes. Thus, both the disorder in the isolated chains as well as the lateral interactions can be investigated. Parameters which are generally used to probe the structure and phase transition in a number of systems containing long n-alkyl chains such as lipid bio-membranes, polymethylene chains as well as mesogens, is the peak intensity ratio of meaningful pairs of C-H stretching bands.

Although such Fermi resonance may affect the distribution of intensity in dramatic ways, it is not expected to significantly affect the total integrated intensity of the fundamentals<sup>24</sup>. The ratio  $I_{2850}/I_{2880}$  is dependent on the lateral order of extended chains. Its use as a measure of lateral disorder is appropriate only in the absence of significant conformational disorder. The value of the ratio is dependent on a number of different factors according to whether or not the chain is extended. In the case of extended chain  $I_{2880}$  consists of approximately equal contribution from  $d^-(o)$  and  $d^+(o)$ .

### Vibrational Modes of the Chelate Ring

If we consider only the benzene rings attached to the chelate ring in Fig. 1 as an approximation similar to the case of Dibenzoylmethane<sup>26</sup>, the molecule can be assigned to have  $C_{2v}$  symmetry implying a single minimum potential. The different internal modes associated with the chelate ring, corresponding to both the  $C_{2v}$  and  $C_s$  configurations<sup>26</sup> are represented in Fig. 2. In the case of a symmetric single minimum potential, a complete delocalisation of the  $\pi$ -electrons of the chelate ring will be expected. As the enolic proton moves away from the  $C_2$  axis towards the oxygen atoms, delocalisation of the  $\pi$ -electrons will be curtailed leading to the formation of double and single bonds.

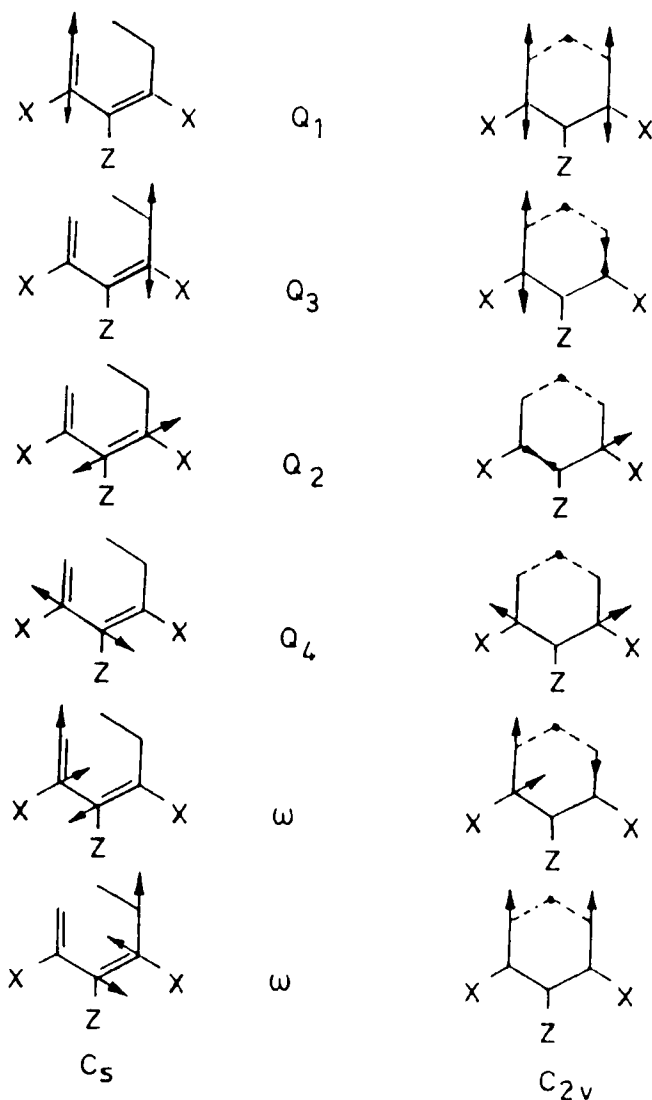


FIGURE 2 A representation of the different internal modes associated with the chelate ring corresponding to both  $C_{2v}$  and  $C_s$  configurations

In the case of a double minimum potential with a high barrier, the proton tunneling frequency ( $\nu_t$ ) is approximately equal to zero and the behaviour of the internal modes of the chelate ring will be the same as in the case of an asymmetric potential. By decreasing the barrier height and allowing the proton to tunnel,



the bands corresponding to these internal modes are expected to split, or more likely produce broadening. When the barrier height is further decreased, the splitting in the bands are expected to increase, with the result that the single and double bond stretching modes approach their corresponding pure stretching modes. The IR and Raman spectra clearly establish the formation of this chelate ring, facilitated by resonance stabilization as evidenced by the absence of any bands in the  $1650\text{--}1800\text{ cm}^{-1}$  corresponding to the free carbonyl modes.

### 3. EXPERIMENTAL

The methods of preparation of these compounds and the characterisation of their mesophases have been reported by Veena Prasad and Sadashiva<sup>24</sup>. For FT-IR measurements, the sample pellets were prepared by dispersing them in a KBr matrix (1:30). FT Raman measurements were carried out on pure samples filled in small capillary tubes. For FT-IR measurements, a resolution of  $1\text{ cm}^{-1}$  and for FT-Raman, an instrument resolution of  $2\text{ cm}^{-1}$  are employed.

### 4. RESULTS AND DISCUSSION

Due to the delocalisation of the  $\pi$ -electrons in the chelate ring<sup>26</sup> and the resonance stabilization thereby, this molecule would prefer the enol form (the vibrational spectra strongly support this and will be discussed later). Because of the planarity of the diketone region of the molecule, the core of this molecule is somewhat rigid about the C  $\alpha$  – position. However, the benzene rings attached to the chelate ring have a rotational degree of freedom about the chelate ring plane along their bonding axis. Because of this, in addition to the conformational changes in the alkyl chains one can expect disorder in the aromatic core of the molecule.

The vibrational spectra of these systems are highly complex due to a large number of fundamentals of the aromatic core, chelate ring and the methylene band progressions. However, most of the specific bands were characterised in comparison with the model compounds like n-alkanes, dibenzoylmethane etc., as reported in literature<sup>4,11–15,18–20,23,25–27</sup>. In addition, it is observed that the vibrational spectra of C<sub>12</sub> is significantly different from those of C<sub>10</sub> and C<sub>11</sub> by the presence of a number of additional bands and splitting.

The C-H stretch regions of the FT-IR and FT-Raman spectra of C<sub>10</sub>, C<sub>11</sub> and C<sub>12</sub> at room temperature are presented in Fig. 3. An assignment of the alkyl

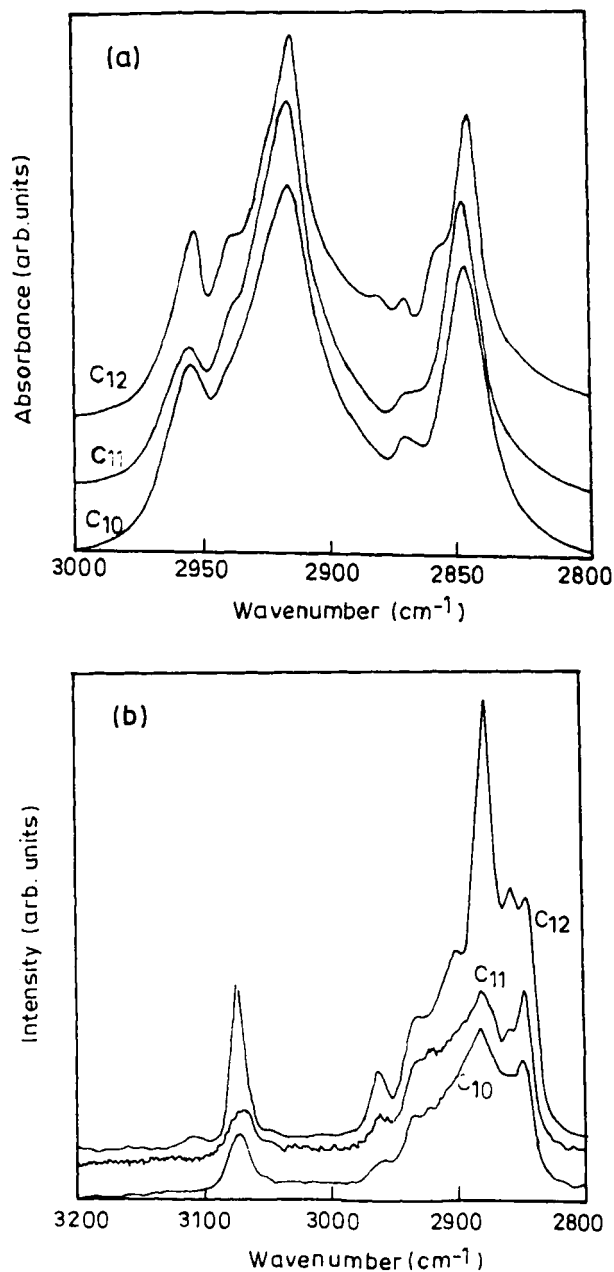


FIGURE 3 The C-H stretch region of (a) The FT-IR spectra and (b) The FT-Raman spectra of C<sub>10</sub>, C<sub>11</sub> and C<sub>12</sub> at room temperature

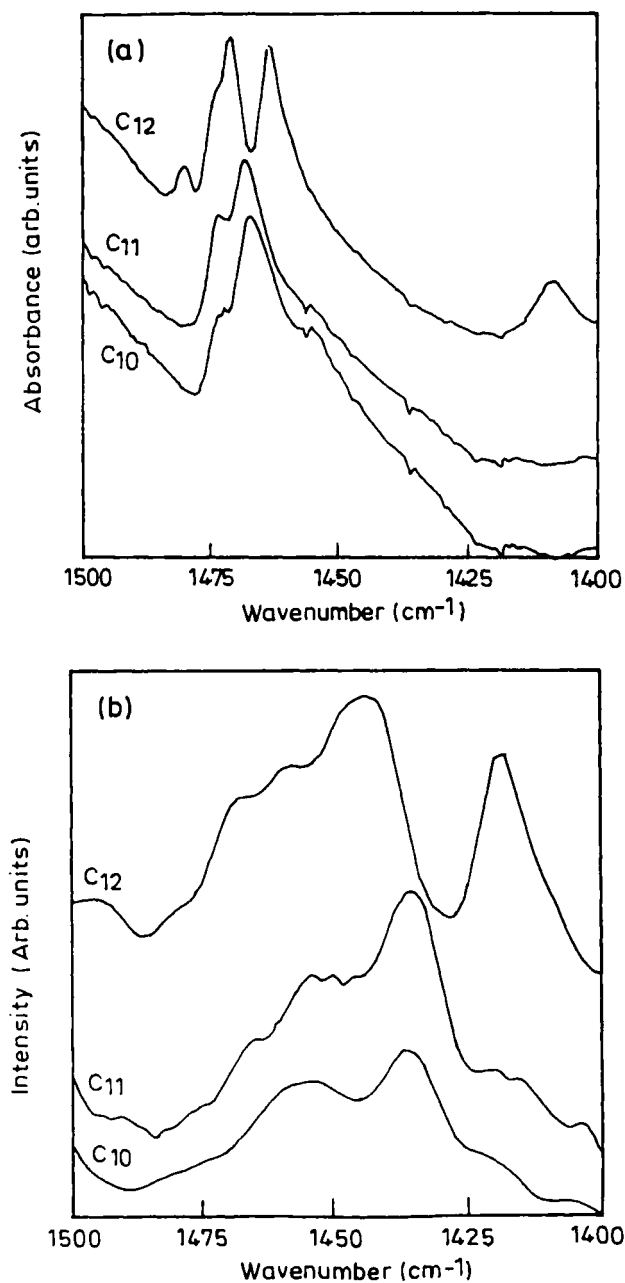


FIGURE 4 (a)The FT-IR spectra and (b)The FT-Raman spectra of C<sub>10</sub>, C<sub>11</sub> and C<sub>12</sub> in the methylene bending region at room temperature

chain modes of  $C_{10}$ ,  $C_{11}$  and  $C_{12}$  is provided in Table I. While both the IR and Raman spectra of  $C_{10}$  and  $C_{11}$  exhibit gross similarities, they differ significantly with the spectra of  $C_{12}$ . These differences are more striking in the Raman spectra of these systems. This is because of the difference in the Fermi resonance interaction of the overtones of the methylene bending modes with the methylene C-H stretch modes and must be originating from the differences in the methylene bending mode frequencies. Such differences in the spectra of these systems must be either due to a prominent change in the conformation of the alkyl chain or a large difference in the degree of intermolecular coupling. Since at low temperatures, all-trans or fully extended conformations are preferred, the drastic change in the Raman spectrum of  $C_{12}$  from those of  $C_{10}$  and  $C_{11}$  arises out of a different degree of lateral interaction of the alkyl chains in these systems and possibly  $C_{12}$  belongs to a different crystal structure. Though such interactions are present in the IR spectra also, they are more prominent in the Raman spectra for the reasons discussed elsewhere<sup>13,15</sup>.

The bands around  $2850\text{ cm}^{-1}$  and  $2880\text{ cm}^{-1}$  in the Raman spectra are assigned to the  $d^+(0)$  and  $d^-(0)$  modes respectively<sup>15</sup>. Generally, the  $d^-$  mode is not expected to show a large degree of Fermi resonance enhancement. The large intensity of the  $d^-$  mode indicates a close crystal packing and possibly a break down of the selection rules though inter-chain coupling. The intensity ratios  $I_{2849}/I_{2880}$  for  $C_{10}$ ,  $C_{11}$  and  $C_{12}$  are 0.83, 0.90 and 0.57 respectively indicating a much higher order in  $C_{12}$ .

## CH<sub>2</sub> bending modes

As discussed earlier, the methylene bending modes are highly sensitive to the intermolecular interactions and conformational changes. Earlier studies<sup>27</sup> in n-alkanes and related systems reveal a large degree of splitting in the CH<sub>2</sub> bending and rocking modes when the chains are packed in the orthorhombic or monoclinic cell. In the hexagonal subcell on the other hand both the symmetry considerations and the inter-chain distances are practically close to that in the liquid and thus rule out splitting. In the triclinic arrangement also only a single component of every fundamental is expected.

The FT-IR and FT-Raman spectra respectively of  $C_{10}$ ,  $C_{11}$  and  $C_{12}$  in the methylene bending region are presented in Fig 4. The IR spectrum of  $C_{10}$  has a strong, broad band at  $1468\text{ cm}^{-1}$  and two weak shoulders on either side at  $1473$  and  $1460\text{ cm}^{-1}$ . The spectrum of  $C_{11}$  is almost similar to that of  $C_{10}$ , but for the relative intensities of the shoulders. The relative intensity of the  $1473\text{ cm}^{-1}$  band with reference to the  $1468\text{ cm}^{-1}$  band is more in the spectrum of  $C_{11}$  compared to that in the spectrum of  $C_{10}$ . In addition, the shoulder at  $1460\text{ cm}^{-1}$  is negligibly weak

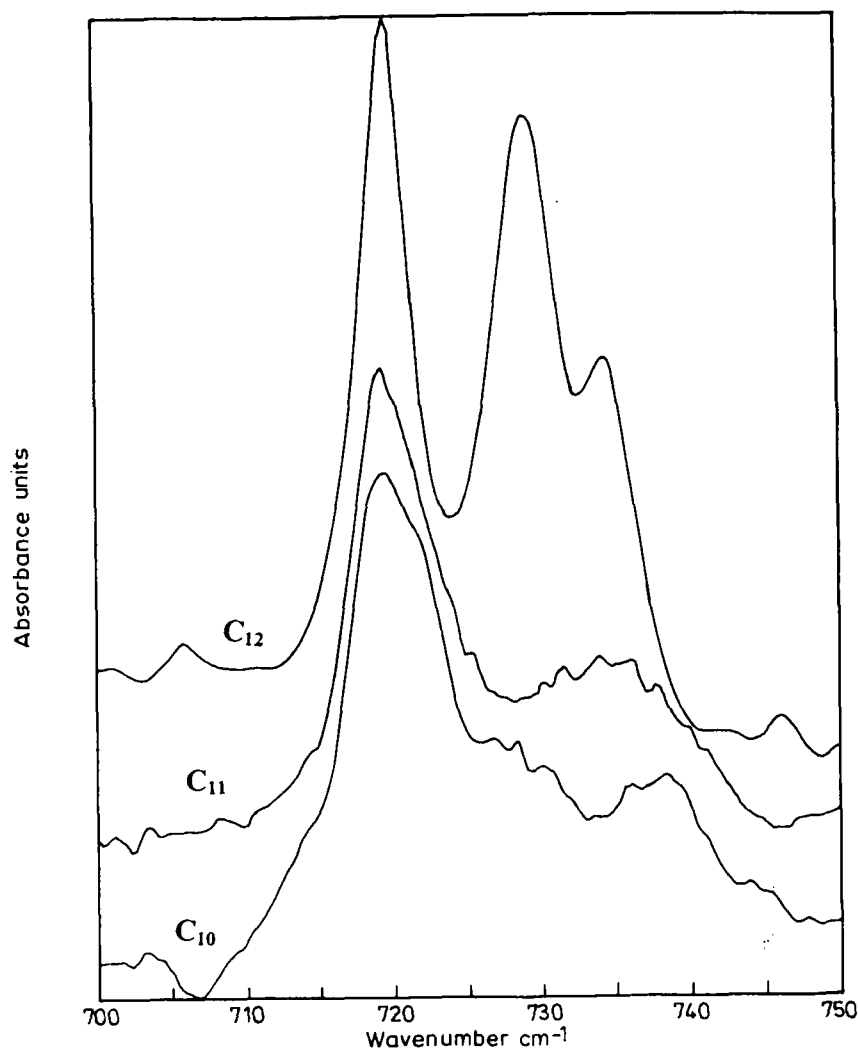


FIGURE 5 The CH<sub>2</sub> rocking region of the FT-IR spectra of C<sub>10</sub>, C<sub>11</sub> and C<sub>12</sub>

in the spectrum of C<sub>11</sub>. However, the spectrum of C<sub>12</sub> is very distinct. It is seen that the CH<sub>2</sub> bending modes are split into two sharp bands of nearly equal intensity appearing at 1471 cm<sup>-1</sup> and 1464 cm<sup>-1</sup>. This splitting of the CH<sub>2</sub> bending modes indicates that the crystal structure of C<sub>12</sub> belongs to the monoclinic or orthorhombic unit cells while those of C<sub>10</sub> and C<sub>11</sub> belong to the hexagonal or triclinic packing<sup>31</sup>.

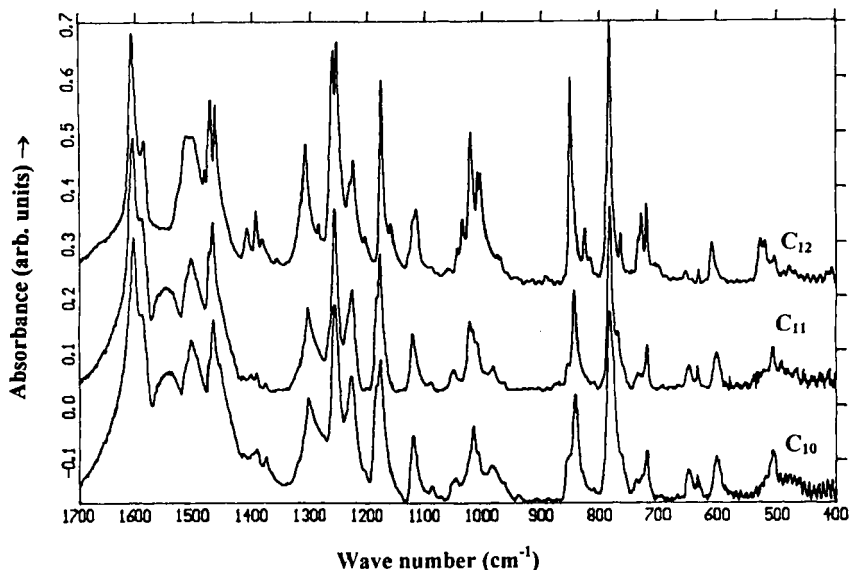


FIGURE 6 The FT-IR spectra of  $C_{10}$ ,  $C_{11}$  and  $C_{12}$  in the region  $400 - 1700 \text{ cm}^{-1}$

The FT-Raman spectrum of  $C_{12}$  also differs largely from those of  $C_{10}$  and  $C_{11}$  in the methylene bending region. It is observed that the  $\delta(0)$  mode is split giving rise to two bands at  $1442$  and  $1415 \text{ cm}^{-1}$ . The spectrum of  $C_{12}$  also shows the presence of two weaker bands at  $1456 \text{ cm}^{-1}$  and  $1468 \text{ cm}^{-1}$ . The two broad bands at  $1435 \text{ cm}^{-1}$  and  $1454 \text{ cm}^{-1}$  in the Raman spectrum of  $C_{10}$  are of nearly equal intensity. On the other hand, the relative intensity of the bands in the  $C_{11}$  spectrum in this region are slightly different from that of  $C_{10}$  indicating a difference in the degree of lateral interaction.

### **CH<sub>2</sub> rocking Modes**

The methylene rocking modes are also sensitive to the crystal structure differences in a similar way as the bending modes. The CH<sub>2</sub> rocking region of the FT-IR spectra of  $C_{10}$ ,  $C_{11}$  and  $C_{12}$  are presented in Fig. 5. The spectra of  $C_{10}$  and  $C_{11}$  resemble each other while the spectrum of  $C_{12}$  is markedly different from the other two. The spectrum of  $C_{10}$  shows a strong band at  $719 \text{ cm}^{-1}$  with a shoulder at  $723 \text{ cm}^{-1}$ . There are two more weak bands at  $728$  and  $738 \text{ cm}^{-1}$  in the spectrum of  $C_{10}$ . The shoulder at  $723 \text{ cm}^{-1}$  present in the  $C_{10}$  spectrum is almost absent in the  $C_{11}$  spectrum. In addition, there is only a single, weak, broad band

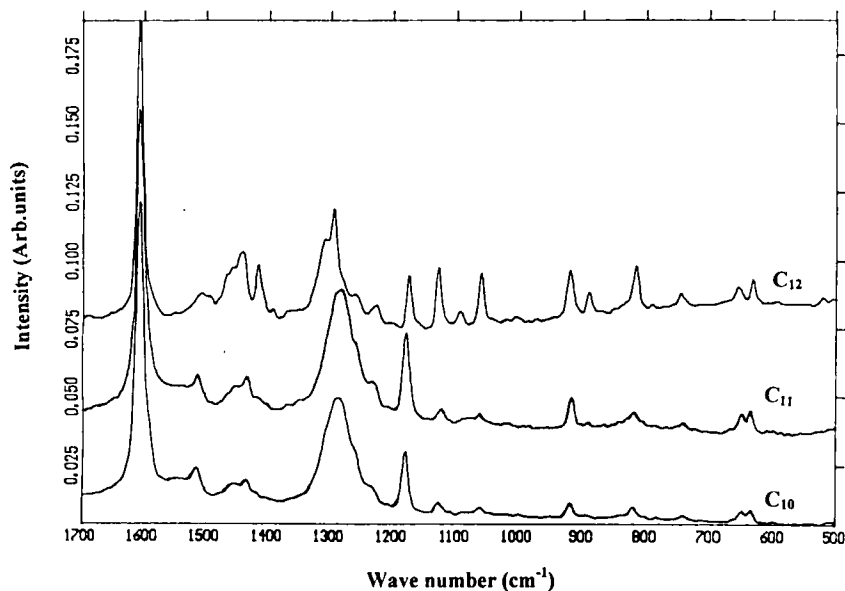


FIGURE 7 The FT-Raman spectra of  $C_{10}$ ,  $C_{11}$  and  $C_{12}$  in the region  $400 - 1700 \text{ cm}^{-1}$

in the spectrum of  $C_{11}$  around  $730 \text{ cm}^{-1}$  other than the  $719 \text{ cm}^{-1}$  band. However, the spectrum of  $C_{12}$  presents strong splitting of the  $\text{CH}_2$  rock modes and two sharp bands of nearly equal intensity are observed at  $719 \text{ cm}^{-1}$  and  $728 \text{ cm}^{-1}$  apart from a relatively weaker sharp band at  $734 \text{ cm}^{-1}$ . The splitting of these bands also strongly supports the supposition that  $C_{12}$  belongs to a crystal structure different from the other two.

Thus an analysis of the C – H stretch,  $\text{CH}_2$  bend and  $\text{CH}_2$  rock regions of the IR and Raman spectra indicate that the crystal structure of  $C_{12}$  is different from those of  $C_{10}$  and  $C_{11}$  and possibly belongs to an orthorhombic or monoclinic packing. On the other hand, the  $C_{10}$  and  $C_{11}$  may belong to a hexagonal packing. A closer look at the spectra of  $C_{10}$  and  $C_{11}$  reveals that although these two compounds probably belong to the same crystal structure, there is definitely a difference in the inter-chain order present in these systems. If  $I_{2880}/I_{2850}$  can be taken as a measure of the lateral order as discussed earlier, the lateral order in  $C_{11}$  appears to be lower than that in  $C_{10}$ . The spectral features of these systems also seem to support this view.

The FT-IR and FT-Raman spectra of  $C_{10}$ ,  $C_{11}$  and  $C_{12}$  in the region  $400 - 1700 \text{ cm}^{-1}$  are given in Fig. 6 and Fig. 7. A tentative assignment of the various bands is presented in Table II. While the spectra of  $C_{10}$  and  $C_{11}$  closely resemble each

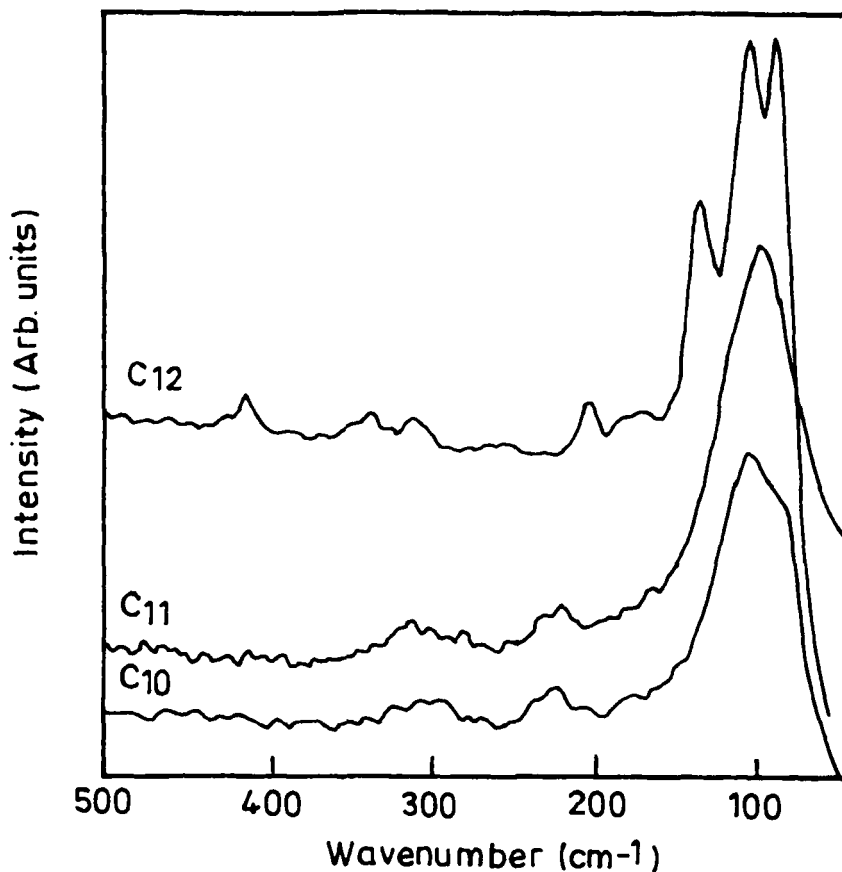


FIGURE 8 The FT-Raman spectra of  $C_{10}$ ,  $C_{11}$  and  $C_{12}$  in the region  $50\text{--}400\text{ cm}^{-1}$

other, that of  $C_{12}$  presents significant differences. The bands in the IR spectrum of  $C_{12}$  are sharper and split when compared to those in the spectra of  $C_{10}$  and  $C_{11}$ . The relative intensities of the various bands in the spectrum of  $C_{12}$  are also different from the spectra of  $C_{10}$  and  $C_{11}$ . The Raman spectrum of  $C_{12}$  is strikingly different from those of  $C_{10}$  and  $C_{11}$  by the presence of a number of additional bands present in it. The presence of these additional bands and the splitting of the bands in both the IR and Raman spectra of  $C_{12}$  strongly suggest that  $C_{12}$  belongs to a highly ordered lattice compared to  $C_{10}$  and  $C_{11}$ .

As discussed earlier, free carbonyl groups are not present in the system as evidenced from the absence of the corresponding bands confirming the formation of



the chelate ring. The band appearing at  $1605\text{ cm}^{-1}$  in the IR spectrum corresponds to the benzene ring symmetric stretch vibration and the shoulder at  $1595\text{ cm}^{-1}$  correspond to the asymmetric ring vibration.

## Low Frequency Region

The Raman spectra of  $C_{10}$ ,  $C_{11}$  and  $C_{12}$  in the  $50\text{--}400\text{ cm}^{-1}$  region are presented in Fig. 8. The spectra of  $C_{10}$  and  $C_{11}$  are almost identical with a strong band at  $108\text{ cm}^{-1}$  and two weak bands at  $224\text{ cm}^{-1}$  and  $300\text{ cm}^{-1}$ . The spectrum of  $C_{12}$  is clearly distinct from those of  $C_{10}$  and  $C_{11}$ . Three strong bands are present at  $92\text{ cm}^{-1}$ ,  $108$  and  $136\text{ cm}^{-1}$  in the room temperature spectrum of  $C_{12}$ . These bands may be due to the internal torsional modes of the alkyl chains and lattice vibrations<sup>4</sup>. The  $C_{12}$  spectrum also has a few weak bands at  $177$ ,  $204$ ,  $312$  and  $339\text{ cm}^{-1}$ . Though an assignment of these bands is not attempted presently, they support the view that the crystal structure of  $C_{12}$  is different from those of  $C_{10}$  and  $C_{11}$ .

## Acknowledgements

The CSIR fellowship for PR is gratefully acknowledged.

## References

1. G.W. Gray, and H. Mosely, *J. Chem. Soc. Perkin Trans.*, **1**, (1974) 97–102.
2. A. H Giroud-Godquin, and P. M. Maithis, *Angew. Chem. Int. Engl.*, **30**, (1991) 375–402.
3. S. A Hudson, and P. M. Maithis *Chem. Rev.*, **93**, (1993), 861–885.
4. Bulkin, B. J. *Appl. Spectrosc.*, **30**, (1976) 261–269.
5. S. Chandrasekhar, B. K. Sadashiva, and K. A. Suresh *Pramana*, **9**, (1977) 471–480.
6. M. Kardan., A. Kaito, S. L. Hsu, R. Thakur, and C. P. Lillya *J. Phys. Chem.*, **91**, (1987) 1809–181.
7. M. Kardan, B. B. Reinhold, S. L. Hsu, R. Thakur, and C. P. Lillya *Macromolecules*, **19**, (1986) 616–621.
8. S. Chandrasekhar, B. R. Ratna, B. K. Sadashiva, and V. N. Raju *Mol. Cryst. Liq. Cryst.*, **165**, (1988) 123.
9. I. Dozov, and N. Kirov. *J. Chem. Phys.*, **90**, (1989) 1099.
10. R. G. Snyder, M. Maroncelli, and H. L. Strauss *J. Am. Chem. Soc.*, **105**, (1983) 133–134.
11. R. G Snyder, and J. H. Schachtschneider, *Spectrochim. Acta*, **19**, (1963) 85–116.
12. R. G. Snyder, *J. Chem. Phys.*, **47**, (1967) 1315–1360.
13. R. G. Snyder and J. R. Scherer *J. R. Scherer J. Chem., Phys.*, **71**, (1979) 3221–3228.
14. R. G. Snyder, H. L. Strauss and C. A. Elliger *J. Phys. Chem.*, **92**, (1982) 5080–5082.
15. R. G. Snyder, S. L. Hsu and S. Krimm, *Spectrochim. Acta.*, **34A**, (1977) 395–405.
16. R. G. Snyder, V. J. P. Srivastavoy., D. A. Cates., H. L. Strauss., J. W. White and D.L. Darset *J. Phys. Chem.*, **98**, (1994) 674–684.
17. M. Maroncelli, H. L. Strauss, and R. G. Snyder *J. Phys., Chem.*, **89**, (1985). 5260–5267.
18. M. Maroncelli, H. L. Strauss, and R. G. Snyder *J. Phys. Chem.*, **82**, (1985), 2811–2824.
19. M. Maroncelli, H. L. Strauss, and R. G. Snyder *J. Phys. Chem.*, **89**, (1985) 4390–4395.
20. M. Maroncelli, S. P. Qi, H. L. Strauss and R. G. Snyder *J. Am. Chem. Soc.*, **104**, (1982) 6237–6247.
21. J. H Schachtschneider., and R.G. Snyder *Spectrochim. Acta*, **19**, (1963) 117–168.
22. Y. Kim, H. L. Strauss, and R. G. Snyder, *J. Phys. Chem.*, **93**, (1984) 485–490.

23. P. Simova, N. Kirov, M. P. Fontana, and H. Ratajczak (eds.), *Atlas of Vibrational Spectra of liquid crystals*, World Scientific, Singapore, 1988.
24. Veena Prasad, and B.K. Sadashiva, *Mol. Cryst. Liq. Cryst.*, **195**, (1991) 161–167.
25. L. Noirez., P. Keller, and J.P. Cotton, *Liquid Crystals*, **18**, (1995) 129–148.
26. S. F. Tayyari, Th. Zeegers-Huyskens, and J. L. Wood, *Spectrochim. Acta*, **35A**, (1979) 1265–1276.
27. T. K. K., Srinivasan, C. I. Jose and A. B. Biswas *Can. J. Chem.*, **47**, (1968) 3877–3891.